INSTITUTE OF PHYSICS PUBLISHING JOURNAL OF PHYSICS: CONDENSED MATTER

J. Phys.: Condens. Matter **18** (2006) 2537–2551 doi:10.1088/0953-8984/18/8/016

Solubility diagram of the Cu–Ni nanosystem

A Shirinyan[1], M Wautelet[2] and Y Belogorodsky[1]

[1] Department of Physics, Cherkasy B. Khmelnytsky National University, 81, Shevchenko street, Cherkasy, 18031, Ukraine
[2] Physics of Condensed Matter, University of Mons-Hainaut, 23, Avenue Maistriau, B-7000 Mons, Belgium

E-mail: shirinyan@phys.cdu.edu.ua and michel.wautelet@umh.ac.be

Received 13 July 2005, in final form 1 December 2005
Published 10 February 2006
Online at stacks.iop.org/JPhysCM/18/2537

Abstract

The application of equilibrium thermodynamics to a nanosystem changes Gibbs's rule of geometrical thermodynamics. This fact leads to the necessity to reconsider the phase diagram and solubility curve concepts. The notions of 'solubility diagram', 'solidus', 'liquidus' are used to discuss the case of phase transition in Cu–Ni nanoparticles. It is shown that, in the limit where thermodynamic arguments remain valid, the solubility diagrams of nanoparticles are functions of their size and nucleation mode. This is demonstrated for different sizes.

1. Introduction

Nanosystems with dimensions in the range 1–100 nm have unique behaviour, related to so-called size effects. Size effects are known to give rise to the shift of the temperature of phase transitions in small particles (like the decrease of the melting temperature with decreasing size) [1–4]. Another effect is observed for first-order phase transformations in binary and multicomponent finite systems, when the atomic composition is varied [5–7]. This is the so-called depletion effect. In the classical nucleation theory, it is assumed that the phase transition takes place in an infinite reservoir, so that there is no problem of matter supply during nucleation. In a nanosystem the total amount of one of the chemical components may be too small for the synthesis of the critical nucleus. Many new examples and works devoted to the mentioned topic were recently published and explained in the framework of classical thermodynamics without taking into account this very important factor [8, 9].

In our previous works, it is argued that, in nanosystems, the concept of equilibrium phase diagram has to be revised. This is due to the fact that the usual concept of phase diagram implicitly assumes that the amount of matter is unlimited. Actually, phase diagrams in nanosystems are not only *shifted*, but are also *split* [10–12], implying the reconsideration of such basic concepts as the phase diagram and solubility curve. In previous works, we outlined the definition of the size-induced 'solubility diagram' and separated it from the definition of the

'phase diagram' (which is now transformed into the 'nanophase diagram') [13]. We proposed to differentiate the solidus and liquidus curves and equilibrium curves after the first-order phase transition and introduced new notions for transforming nanosystems [13]. While the theoretical approach has a rather general character, one can report some specific applications of experimental interest. In this respect, isolated nanoparticles of Pb–Bi alloys have size-induced melting behaviour, recently observed by hot stage transmission electron microscopy [11].

Furthermore, we want to elucidate the qualities of possible effects on the phase transition and state diagrams in the Cu–Ni nanosystem. The aim of the present work is to describe the 'solubility diagram' for the particular case of Cu–Ni isolated nanoparticles, related to the non-negligible depletion effect. Hereby we restrict ourselves to the thermodynamic study of melting and freezing. We treat cases where the thermodynamic approach remains valid. This implies that: (1) the overall radius of the nanoparticle is relatively large ($R \geqslant 2$ nm; the total number of atoms is much larger than a few hundred atoms), (2) the surfaces of the core and the shell are characterized by a single values of the surface tension, and (3) the temperature, T, is an appropriate parameter to describe the state of the particle and is valid for the study of nanoparticles in thermal equilibrium.

Recent molecular dynamics simulations show that in binary nanoparticles the interplay of structure and chemical ordering (segregation) may be crucial for determining the melting temperature [14–16]. In the specific case of Cu–Ni nanoclusters, melting may occur in two stages: first, the external copper shell melts and the nickel core remains solid, then the nickel core melts [17]. In the following, the effect of segregation on the melting temperature is not considered; that is, near the melting temperature the given metals, Cu and Ni, are assumed to be perfectly mixed in the nanoparticle.

The structure of the paper is as follows. In section 2 we shortly recall the new proposed definition of 'solubility diagram' for transforming binary and multicomponent nanosystems. Then we discuss the different evolution paths (modes) of transforming a nanoparticle and define the transition criterion (section 3). In section 4 thermodynamic potentials for the Cu–Ni system are introduced. Here we also outline the thermodynamics of melting and freezing of an isolated Cu–Ni nanoparticle for each mentioned mode. The results of the optimization procedure are presented in section 5. In section 6 we give a summary and concluding remarks.

2. Solubility diagram

Let us first review what the size-induced solubility diagram is [13]. To do this, first we recall the solubility curve notions, namely, the 'liquidus' and 'solidus'. The liquidus curve is *'in a temperature–concentration diagram, the line connecting the temperatures at which* ***freezing*** *is just* ***started*** *for various compositions of a starting liquid phase'*. In a similar way, the solidus is the solubility curve for a solid nanosystem. Hence the solidus curve is the *'curve representing in a temperature–concentration diagram, the line connecting the temperatures at which* ***fusion*** *is just* ***started*** *for various compositions of a starting solid phase'*.

Let us now introduce the 'solubility limits' notion. Under the solubility or solubility limits we understand the limit compositions at which the starting (single-phase) state remains without transition into another (two- or multi-phase) state. By varying the initial composition, x_0, and the temperature, T, one can find that the solubilities gather into solubility curves (in our case, liquidus and solidus).

In the case of a nanoparticle, when we want to find the solidus, we start from the initial totally solid particle, as a single phase state, and calculate the solid to liquid transition. The solubility limit in this case is the limit composition of one of the components at which the solid-to-liquid transition *starts*. Then by plotting the corresponding points as a temperature–

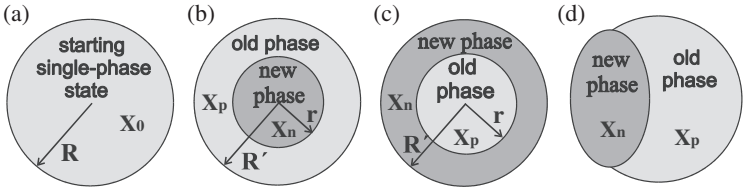

Figure 1. Different transition modes. Qualitative representation of a nanoparticle of initial composition x_0 before phase transition (a) and the same transformed nanoparticle after ((b)–(d)): x_p—composition of the old phase after the transition, x_n—composition of new-born phase, r—new phase nucleus size (b) and radius of the parent phase (c), R and R'—radii of nanometric particle before nucleation and after the transformation, respectively.

composition diagram we obtain the curve, and at least, the diagram of solubility in the solid substance (with solidus). The same reasoning is applicable to the liquidus curve.

We define the solubility diagram as follows: the *'solubility diagram is the temperature–composition diagram at fixed quantity of matter of a nanosystem obtained by plotting the solubility curves'*. Solubility curves will not explain the usual equilibrium conditions [13]. Nevertheless, such a definition of the solubility diagram is very similar to the one of a phase diagram because it describes the phase fields (single solid phase state, single liquid phase state and two-phase states) separated by solubility curves for different initial compositions and temperatures.

Moreover, for a nanosystem, there may exist several lines of solidus (and liquidus), which may be gathered into one curve (shown below). Also, the solidus and liquidus lines may even intersect each other depending on the size of the nanosystem and the mechanism of nucleation of a new phase during the processes of melting and freezing.

Let us apply these notions to the case of transforming an isolated nanoparticle.

3. Transition modes: transition criterion

One must differentiate the solid-to-liquid transition and the liquid-to-solid transition. In the following, the starting single phase is called the 'old' or 'parent' phase and the new formed phase is called the 'new' one. In general, for melting and freezing of a nanoparticle, there may be six quite different transformation modes (figure 1).

3.1. Modes of solid to liquid–solid transition

Let us start from a solid particle of initial composition x_0 and go from low to high T (figure 1(a)). Then the indication of melting will be the appearance of a liquid (two-phase solid–liquid state). This is the solidus temperature and solidus composition x_0. Hereby three transition modes are possible from a pure solid nanoparticle to a liquid–solid configuration of the nanoparticle (figure 1):

(i) the liquid part appears in the shell of the particle (figure 1(c));
(ii) the liquid part appears in the core of the particle (figure 1(b));
(iii) the liquid part appears at the external boundary of the particle, at the interface ('liquid cap') (figure 1(d)).

Here, the 'new' phase is the formed liquid part of the nanoparticle with composition x_n and the 'parent' one is the solid part of the same nanoparticle with another composition x_p.

3.2. Modes of liquid to liquid–solid transition

If one starts from a pure liquid particle at high T and decreases T, then freezing takes place. So the corresponding liquidus temperature (and the composition in the starting phase) indicates the appearance of a solid part in a nanoparticle. Here, the 'new' phase is the formed solid part of the nanoparticle with composition x_n and the 'parent' one is the liquid part of the same nanoparticle which has another composition x_p.

In a way similar to the above-mentioned modes, the liquid to liquid–solid transition has three different paths. Again, three principally different geometric configurations are possible from a pure liquid single-phase nanoparticle to a liquid–solid two-phase nanoparticle (figure 1):

(iv) the solid part appears in the shell of the particle (figure 1(c));
(v) the solid part appears in the core of the particle (figure 1(b));
(vi) the solid part appears at the external boundary of the particle, at the interface ('solid cap') (figure 1(d)).

One must investigate the thermodynamics of all six cases separately (section 5).

3.3. Transition criterion

The condition that the Gibbs free energy of the total system for the new (two-phase) configuration (figures 1(b)–(d)) is smaller than for the starting (single-phase) one (figure 1(a)), is taken as the transition criterion. This definition is applied to freezing of a supersaturated liquid nanoparticle as well as for melting of a supersaturated solid nanoparticle [10, 12].

The corresponding thermodynamic analysis clearly shows that after the transition (in each mode), one can find the optimal compositions corresponding to the phase transition criterion [10, 12, 13]. Actually, we have always three characteristic points: (1) *initial* composition x_0 as the limit of solubility of one component in another; (2) composition x_p of the depleted ambient parent phase *after* the phase transition; (3) composition x_n of the new-born phase as the result of the phase transition.

In usual phase diagram methods, the compositions of the liquid and solid phases are given by the compositions, at fixed T, of the liquidus and solidus curves. However, the amount of matter in the nanoparticle is limited. So, the corresponding stoichiometry of the new phase embryo cannot be attained. In other words, compositions x_n, x_p, x_0 are different because of the above-mentioned depletion and finite size of the system. So, phase diagrams in nanosystems are split. This fact leads to the necessity to reconsider the phase diagram and solubility curve concepts [13].

In the following we discuss only the solubility diagram. For a solubility diagram we do not need all these optimal compositions [13]. To plot a solubility diagram, we need only the *initial* composition x_0 as the limit solubility of one component in another when the transition criterion is being fulfilled. Even in this case there exists the problem of choice of which solubility line must be taken as the main one.

Let us apply this general result to the particular case of a Cu–Ni nanoparticle.

4. Thermodynamics of phase transition of a Cu–Ni nanoparticle

It is well known that the Cu–Ni system has a lens-type liquidus/solidus bulk diagram (or so-called 'cigar'-type solubility behaviour similar to the Au–Ag, Ge–Si or Nb–W systems) [18, 19]. In the thermodynamic approach this system is described in the framework of the regular solution model [20, 21].

In the regular solution model probabilities of atom arrangement coincide with the concentration of the components [20, 21]. In our case (fixed P and T) the thermodynamic potential will be the Gibbs free energy. The Gibbs free energy of a nanosystem is the sum of two parts: the bulk thermodynamic potential contribution and the surface energy contribution.

4.1. Bulk thermodynamic potentials

Let Δg be the Gibbs free energy density (energy per atom) of formation of the compound: a liquid $\Delta g_{\mathrm{L}}(x,\ T)$; and a solid $\Delta g_{\mathrm{S}}\ (x,\ T)$, respectively. At the liquid–solid transition temperature T the difference in Gibbs free energy densities may be found by the melting enthalpy, entropy and the melting temperature. For the Cu–Ni system, the bulk driving forces $\Delta g_{\mathrm{S}}(x,\ T)$ and $\Delta g_{\mathrm{L}}(x,\ T)$ are given by:

$$\Delta g_{\mathrm{S}}(x,T) = x(1-x)\Delta h_{\mathrm{S}} + kT\{x\ln(x) + (1-x)\ln(1-x)\} + p\{(1-x)v_{\mathrm{A}}^{\mathrm{S}} + xv_{\mathrm{B}}^{\mathrm{S}}\}, \quad (2)$$

$$\begin{aligned}\Delta g_{\mathrm{L}}(x,T) = {} & x(1-x)\Delta h_{\mathrm{L}} + kT\{x\ln(x) + (1-x)\ln(1-x)\} \\ & + p\{(1-x)v_{\mathrm{A}}^{\mathrm{L}} + xv_{\mathrm{B}}^{\mathrm{L}}\} + x\Delta h_{\mathrm{m,B}}(T_{\mathrm{m,B}} - T)/T_{\mathrm{m,B}} \\ & + (1-x)\Delta h_{\mathrm{m,A}}(T_{\mathrm{m,A}} - T)/T_{\mathrm{m,A}}. \end{aligned} \quad (3)$$

Here, $\Delta h_{\mathrm{m,B}}$, $T_{\mathrm{m,B}}$, $\Delta h_{\mathrm{m,A}}$ and $T_{\mathrm{m,A}}$ are the melting enthalpy and bulk melting temperature for B and A atoms, respectively. Δh_{S} is the mixing energy or enthalpy of solid solution formation, Δh_{L} is the enthalpy of formation of the liquid solution. Again, $v_{\mathrm{A}}^{\mathrm{S}}$, $v_{\mathrm{B}}^{\mathrm{S}}$, $v_{\mathrm{A}}^{\mathrm{L}}$ and $v_{\mathrm{B}}^{\mathrm{L}}$ are the atomic volumes of A (Cu) and B (Ni) atoms in the solid and liquid states, respectively. We use Vegard's law for atomic volumes of compounds. In the following the indices L and S refer to the liquid and solid, respectively.

4.2. Interfacial thermodynamic potential

The second term in the Gibbs free energy of a nanosystem is related to the surface energy. In the case of metals and alloys, the surface energy σ is not obtained directly. We estimate the value $\sigma(x)$ for a metallic binary alloy and binary liquid of the Cu–Ni system in the framework of ideal and regular solution models. Also, the value σ is taken to be equal to the surface tension. Consider the binary system consisting of species A and B. Writing only the first main terms in a Taylor's series $\sigma(x)$ from x, one obtains the linear function $\sigma(x)$ for a solid as well as for a liquid:

$$\sigma_{\mathrm{L}}(x) = x\sigma_{\mathrm{B}}^{\mathrm{L}} + (1-x)\sigma_{\mathrm{A}}^{\mathrm{L}} \quad (4a)$$

$$\sigma_{\mathrm{S}}(x) = x\sigma_{\mathrm{B}}^{\mathrm{S}} + (1-x)\sigma_{\mathrm{A}}^{\mathrm{S}}. \quad (4b)$$

This approach is analogous to Vegard's law for the atomic density of compounds.

4.3. Interphase tension between two phases

The specific interfacial energy between two macroscopic phases with different compositions x_1 and x_2 has been taken as the difference between the specific interfacial energies of the phases. So, in our case of liquid–solid interface one should write:

$$\sigma_{\mathrm{SL}}(x_1, x_2) = \sigma_{\mathrm{LS}}(x_1, x_2) = |\sigma_{\mathrm{S}}(x_1) - \sigma_{\mathrm{L}}(x_2)|. \quad (5)$$

From a qualitative point of view, the estimation (5) is related to the coherence between the solid phase and the liquid phase yielding a small interphase energy σ_{SL}.

Under the chosen condition (5) for the value $\sigma_{SL}(x_1, x_2)$, the case (d) in figure 1 is excluded. (This is related to the condition of mechanical equilibrium of phases in the particle.) The configuration (d) in figure 1 transforms into (b) or (c) in figure 1 depending on the sign of the difference $\sigma_S(x_1) - \sigma_L(x_2)$. This means that in our chosen case of Cu–Ni nanosystem the mentioned six modes reduce into four: namely, (i), (ii), (iv) and (v) (see section 3).

Furthermore, the appearance of the new phase is related to the change of atomic densities n of materials and the sizes of the Cu–Ni nanoparticle. To take this into account, one should use the density value n as a function of composition and state of the phase in the following way:

$$n_S(x) = 1/\{(1-x)v_A^S + x v_B^S\} \tag{6a}$$

$$n_L(x) = 1/\{(1-x)v_A^L + x v_B^L\}. \tag{6b}$$

In fact, in the case of the Cu–Ni nanosystem the last equations are not important (with respect to our results) due to very small difference in the atomic densities of Cu and Ni.

In the next step, we consider the different modes of transition of a binary Cu–Ni nanoparticle and write the corresponding thermodynamic approach. Let us consider the thermodynamics of each mode more properly and then use the transition criterion for transforming a nanoparticle (section 3).

4.4. Mode (i) of solid → liquid–solid transition (figure 1(c))

At the starting state the Gibbs free energy of a pure solid nanoparticle is given by:

$$G_{0S}(x_0, R) = N\Delta g_S(x_0, T) + \sigma_S(x_0)S_0. \tag{7}$$

In the case of a spherical particle the total number of atoms N and the surface area S_0 are defined as $N = 4\pi n_S(x_0)R^3/3$ and $S_0 = 4\pi R^2$.

The Gibbs free energy of the two-phase Cu–Ni nanoparticle related to the formation of a liquid shell of thickness h and composition x_n is:

$$G_1(x_n, h) = N_S\Delta g_S(x_p, T) + N_L\Delta g_L(x_n, T) + \sigma_{SL}(x_n, x_p)S_{SL} + \sigma_L(x_n)S_L. \tag{8}$$

Here, $N_S = 4\pi n_S(x_p)r^3/3$, $N_L = 4\pi n_L(x_n)[(r+h)^3 - r^3]$, $S_{SL} = 4\pi r^2$, $S_L = 4\pi(r+h)^2$, $\sigma_{SL}(x_n, x_p) = |\sigma_S(x_p) - \sigma_L(x_n)|$, where r is the external radius of the parent solid phase.

The change in Gibbs free energy ΔG_1 of the system is then:

$$\Delta G_1(x_n, h) = G_1(x_n, h) - G_{0S}(x_0, R). \tag{9}$$

Equation (9) implies that the Gibbs free energy change of the system is a function of two variables: x_n (concentration in the new liquid phase) and h (thickness of the liquid shell).

The mass conservation law and the configuration of the Cu–Ni nanosystem lead to an interrelation of mole fractions x_n and x_p, the atomic densities $n_S(x_p)$ and $n_L(x_n)$, the sizes R, r and thickness h by the system of equations:

$$n_S(x_0)R^3 = n_S(x_p)r^3 + n_L(x_n)[(r+h)^3 - r^3], \tag{10a}$$

$$x_0 n_S(x_0)R^3 = x_p n_S(x_p)r^3 + x_n n_L(x_n)[(r+h)^3 - r^3]. \tag{10b}$$

The second term in equation (10*b*) represents the depletion effect. Having h and x_n as the variable parameters one can find r and x_p as their functions at fixed other parameters (R, x_0, T and others).

Let us now look at the equilibrium. To determine the extreme points of the phase transition, one has to consider the variational procedure and solve equations (9), (10) with respect to x_n and h. The value x_0 at the transition criterion represents the solubility in the solid Cu–Ni nanoparticle at fixed T (subsequently referred to as x_{01}).

4.5. Mode (ii) of solid → liquid–solid transition (figure 1(b))

At the starting state the Gibbs free energy of a pure solid nanoparticle is given by formula (7).

The Gibbs free energy of the Cu–Ni nanoparticle in the configuration shown in figure 1(b) can be determined as:

$$G_2(x_n, r) = N_S \Delta g_S(x_p, T) + N_L \Delta g_L(x_n, T) + \sigma_{SL}(x_n, x_p) S_{SL} + \sigma_S(x_p) S_S. \tag{11}$$

Here $N_S = 4\pi n_S(x_p)\{(R')^3 - r^3\}/3$, $N_L = 4\pi n_L(x_n) r^3/3$, $S_{SL} = 4\pi r^2$, $S_S = 4\pi (R')^2$, $\sigma_{SL}(x_n, x_p) = |\sigma_S(x_p) - \sigma_L(x_n)|$, where R' is the radius of the nanoparticle after the phase transition (which may differ from R due to a difference in atomic density). The change in Gibbs free energy in this mode is expressed as:

$$\Delta G_2(x_n, r) = G_2(x_n, r) - G_{0S}(x_0, R). \tag{12}$$

The Gibbs free energy change of the system is a function of x_n and r (radius of the liquid core).

The conservation law yields:

$$n_S(x_0) R^3 = n_S(x_p)\{(R')^3 - r^3\} + n_L(x_n) r^3, \tag{13a}$$

$$x_0 n_S(x_0) R^3 = x_p n_S(x_p)\{(R')^3 - r^3\} + x_n n_L(x_n) r^3. \tag{13b}$$

Using a numerical solution of equations (12), (13) with respect to x_n and r, we find the $\Delta G_2(x_n, r)$ function at other parameters known and fixed. At the transition criterion the minimum of $\Delta G_2(x_n, r)$ is reached. Hereby the value x_0 represents the solubility limit at fixed T (subsequently referred to as x_{02}). The results of such an analysis are presented in the next paragraph.

4.6. Mode (iv) of liquid → solid–liquid transition (figure 1(c))

Formally this mode can be easily determined similarly to the first mode (i). One must only change the indices corresponding to the solid substance into indices for the liquid one and vice versa; that is, L → S and S → L in formulae (7)–(10). Doing this, we find the energy of the starting liquid particle $G_{0L}(x_0, R)$, then the $\Delta G_3(x_n, h)$ function for the nucleation of the solid shell at the interface of the nanoparticle:

$$\Delta G_3(x_n, h) = G_3(x_n, h) - G_{0L}(x_0, R). \tag{14}$$

The minimization procedure at the transition criterion gives the solubility value x_0 at fixed T (subsequently referred to as x_{03}).

4.7. Mode (v) of liquid → solid–liquid transition (figure 1(b))

The same reasoning is applied to this mode, when the solid nucleus appears inside the liquid nanoparticle, in the core. Changing the indices L and S in formulae (7) and (11)–(13), one can analyse the change of the Gibbs free energy $\Delta G_4(x_n, r)$ of the transforming Cu–Ni nanoparticle:

$$\Delta G_4(x_n, r) = G_4(x_n r) - G_{0L}(x_0, R). \tag{15}$$

Again, by the minimization procedure, at transition criterion we obtain the solubility x_0 at fixed T (subsequently referred to as x_{04}).

Let us discuss the conditions for the minimal energy of a given system. It is known that the equilibrium is related to the concavity (or convexity) of thermodynamic potentials [20, 21]. To describe the phase coexistence one should consider the relations between the Gibbs potentials $\Delta g_L(x, T)$, $\Delta g_S(x, T)$ and Gibbs free energies of the system ΔG: $\Delta G_1(x_n, h)$, $\Delta G_2(x_n, r)$, $\Delta G_3(x_n, h)$ and $\Delta G_4(x_n, r)$ with respect to the variable parameters x_n and r or h. Such

Table 1. Thermodynamic data of the binary Cu–Ni solution.

	Cu–Ni system [23–27]	
Quantity/property	Cu	Ni
Structure	fcc	fcc
Atomic mass, M (kg mol^{-1})	63.55×10^{-3}	58.71×10^{-3}
Bulk melting temperature, T_{m}	$T_{\mathrm{m,A}} = 1357$ K (1084 °C)	$T_{\mathrm{m,B}} = 1728$ K (1455 °C)
Atomic volume, v^{S} ($v_{\mathrm{A}}^{\mathrm{S}}$ or $v_{\mathrm{B}}^{\mathrm{S}}$) (m^3)	$v_{\mathrm{A}}^{\mathrm{S}} = 1.181 \times 10^{-29}$	$v_{\mathrm{B}}^{\mathrm{S}} = 1.10 \times 10^{-29}$
Atomic volume, v^{L} ($v_{\mathrm{A}}^{\mathrm{L}}$ or $v_{\mathrm{B}}^{\mathrm{L}}$) (m^3)	$v_{\mathrm{A}}^{\mathrm{L}} = 1.362 \times 10^{-29}$	$v_{\mathrm{B}}^{\mathrm{L}} = 1.253 \times 10^{-29}$
Relative volume change during the melting, $(v^{\mathrm{L}} - v^{\mathrm{S}})/v^{\mathrm{S}}$	4.2%	4.5%
Atomic density of solid, n_{S} (m^{-3})	$n_{\mathrm{A}}^{\mathrm{S}} = 1/v_{\mathrm{A}}^{\mathrm{S}} \approx 8.482 \times 10^{28}$	$n_{\mathrm{B}}^{\mathrm{S}} = 1/v_{\mathrm{B}}^{\mathrm{S}} \approx 9.132 \times 10^{28}$
Atomic density of liquid, n_{L} (m^{-3})	$n_{\mathrm{A}}^{\mathrm{L}} = 1/v_{\mathrm{A}}^{\mathrm{L}} \approx 7.344 \times 10^{28}$	$n_{\mathrm{B}}^{\mathrm{L}} = 1/v_{\mathrm{B}}^{\mathrm{L}} \approx 7.981 \times 10^{28}$
Mass density of solid (kg m^{-3})	8.95×10^3	8.9×10^3
Mass density of liquid (kg m^{-3})	7.75×10^3	7.78×10^3
Mixing energy of solid, Δh_{S} (J)	2.08×10^{-20}	
Mixing energy of liquid, Δh_{L} (J)	2.18×10^{-20}	
Heat of fusion, Δh_{m}($\Delta h_{\mathrm{m,B}}$ or $\Delta h_{\mathrm{m,A}}$) (J mol^{-1})	$\Delta h_{\mathrm{m,A}} = 13050$	$\Delta h_{\mathrm{m,B}} = 17470$
Surface tension of solid, σ_{S} (J m^{-2})	$\sigma_{\mathrm{A}}^{\mathrm{S}} = 1.731$	$\sigma_{\mathrm{B}}^{\mathrm{S}} = 2.243$
Surface tension of liquid, σ_{L} (J m^{-2})	$\sigma_{\mathrm{A}}^{\mathrm{L}} = 1.321$	$\sigma_{\mathrm{B}}^{\mathrm{L}} = 1.768$
Debye temperature (K)	315	375
Size of particle, R (m)	$R_1 = 3 \times 10^{-8}$, $R_2 = 30 \times 10^{-8}$	

analyses have been done by two of the authors in a previous work ([12], and references therein). Also, an equivalent way to describe the equilibrium phase coexistence is to introduce chemical potentials [20–22]. In the present study, extremes of the ΔG function in equations (9), (12), (14), (15) have been found by the direct calculation of ΔG for all reasonable compositions x_{n} and sizes r or h (with small step).

The details needed for the calculations of transforming a Cu–Ni nanoparticle are given in table 1.

The values Δh_{L} and Δh_{S} are taken to be equal to the bulk phase diagram values, in accordance with the well-known experimental data for bulk materials [18, 19].

5. Results: solubility diagram and the problem of choice

As seen in the previous sections, the limited volume of the transforming compound can change the results of decomposition. One can expect interesting possibilities if the nanoparticle transforms due to different modes. In principle, different possibilities (modes considered) give different values of solubility at the same initial set of parameters.

Obviously, the following question arises: which mode is kinetically possible? Or what kinetic mechanism gives priority to one mode with respect to another one? In the present study, the kinetic aspect is not considered. So, in the next thermodynamic approach we have to choose which mode is thermodynamically most advantageous and solve the optimization problem.

In the framework of the classical theory of nucleation, the nucleation rate is given by [20, 21, 28]:

$$J = J_0 \exp\{-\Delta G^*/kT\} \exp\{-\Delta G_{\mathrm{D}}/kT\}. \tag{16}$$

Here J is the steady-state rate of formation of the 'new' phase (thermodynamically stable with respect to the initial state), J_0 is a frequency constant, ΔG^* is the nucleation barrier, and ΔG_{D} is the activation energy for diffusion across the parent phase–nucleus interface.

Let ΔG_i^* be the nucleation barrier corresponding to the transition criterion at solubility x_{0i} (i is the number of the mentioned mode, $i = 1, 2, 4, 5$) and the same initial parameters (table 1). According to (16) the process is controlled by both the thermodynamic and the kinetic energy barriers of nucleation. Assuming that ΔG_{D} is the same for different modes (there are no kinetic constraints), $\Delta G_i^* < \Delta G_j^*$ ($i \neq j$, $j = 1, 2, 4, 5$) implies that $J_i > J_j$. This means that from all existing possibilities for x_{0i} one must choose the one with the highest probability, greatest nucleation rate and smallest nucleation barrier.

Furthermore, the solubility found by the transition criterion represents the supersaturated condition of the nanosystem when, in principle, the transition may start. So the inequality $\Delta G_i^* < \Delta G_j^*$ ($i \neq j$) implies that the solubility limit x_{0i} (for mode i) is more probable than the solubility limit x_{0j} (for mode j) and the transition will take place via mode i. At the same time, if one increases the initial supersaturation in mode j, then the corresponding nucleation barrier ΔG_j^* decreases. At least, one can find the new values x_{0j} and ΔG_j^* so that $\Delta G_j^* = \Delta G_i^*$. In the last case both modes become equally probable. Then, again, the problem of choice appears: which one (x_{0i} or new found x_{0j}) must be plotted in the solubility diagram and what is the solubility in this Cu–Ni nanoparticle? The answer is the following. The solubility, at fixed T and other parameters, is the one which corresponds to the lower initial supersaturation of the system, that is when the transition starts earlier. In other words, if one starts from a pure solid particle, then for two values x_{0i} and x_{0j} (at the same barriers $\Delta G_j^* = \Delta G_i^*$) the solubility will be that which is closer to the field of the single solid phase state in the solubility diagram. A similar reason is applied to the case of the initially liquid particle.

Also, one more problem needs to be discussed here. Note that the transition criterion at equilibrium (with $\Delta G = 0$ at $r = 0$ and $\Delta G \leqslant 0$ at some $r > 0$) in a small particle may mean two valleys (in Gibbs free energy dependence on radius r), which are separated by a thermodynamic barrier [10, 12]. The results show that in the case of a small Cu–Ni particle this mentioned energy barrier may be high ($>50kT$). From the experimental point of view, this means that the phase transition may not take place even at the transition criterion because of the high barrier. So, one must define also the additional condition at $\Delta G^* \leqslant 50kT$ at $r > 0$ corresponding to the transition criterion. The results are shown in figures 2, 3. In table 2 we introduce the definitions of each transition mode with the corresponding transition criterion to simplify the understanding of subsequent figures.

5.1. Solid to liquid–solid transition

Consider at first solubilities in the modes (i) and (ii), that is for the solid to liquid–solid transition. They are shown in figure 2. As can be seen, for the Cu–Ni system, at the same T and other fixed parameters, there exist different values of x_0.

Let us briefly discuss figure 2. Here we start from the solid particle at low T and then increase T, at fixed R and x_0. When going to high T, a liquid embryo is assumed to be formed inside the nanoparticle (figures 1(b), (c)). This event indicates the occurrence of nucleation. That is, the two-phase liquid–solid configuration of the nanoparticle has minimum of Gibbs energy lower than the one at the initial single-phase solid state. That is the transition criterion. Since the radius of the nanoparticle is small, the solidus lines are size-dependent and shifted, as compared with the bulk one.

Let us now chose which mode, from the four mentioned in table 2 and shown in figure 2, is thermodynamically most advantageous; which has the biggest probability. Doing this, we find that the most probable mode is the one in the case of the newly formed configuration denoted by symbols □ and ○ in figure 2 and table 2: solid core and liquid shell. This leads to the fact that clusters should melt at the surface first (so that the good thermodynamic configuration is

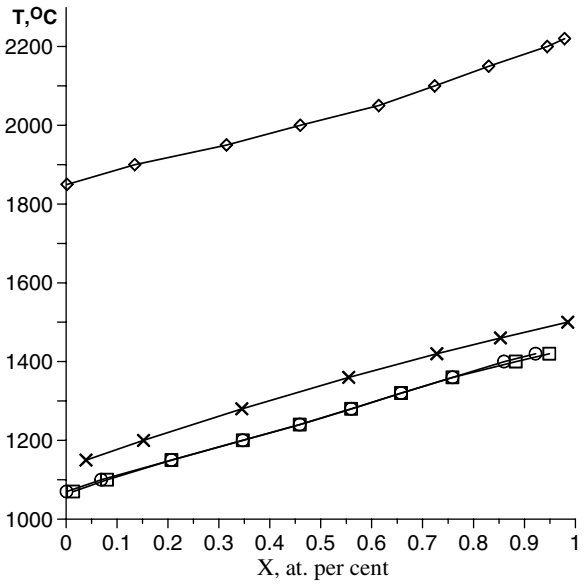

Figure 2. Solidus lines for the different modes of melting at the transition criterion for a Cu–Ni nanoparticle of size R_1. Explanation is given in the text.

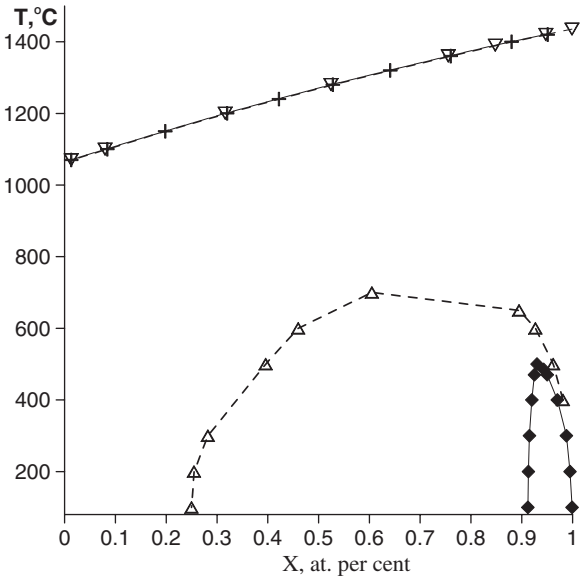

Figure 3. Solubility limits—'liquidus' in a Cu–Ni nanoparticle of size R_1 for the different modes of crystallization. Explanation is given in the text and table 2.

solid core–liquid shell) and the nanoparticle surface is easier to disorder than the inner part. This result, when the liquid coats the solid part, coincides with the well-known wetting effect related to the small value of surface tension of a liquid with respect to that for a solid (table 1).

Table 2. Symbols related to the transition mode and explanation.

Mode	Symbol in figures	The two-phase configuration (figure 1).	Chosen energy criterion
		Starting solid nanoparticle	
i	□	Solid core and liquid shell (figure 1(c))	Transition criterion
	○	Solid core and liquid shell (figure 1(c))	Transition criterion and energy barrier less than $50kT$
ii	×	Liquid core and solid shell (figure 1(b))	Transition criterion
	◇	Liquid core and solid shell (figure 1(b))	Transition criterion and energy barrier less than $50kT$
		Starting liquid nanoparticle	
v	∇(▼)	Solid core and liquid shell (figure 1(b))	Transition criterion
	Δ	Solid core and liquid shell (figure 1(b))	Transition criterion and energy barrier less than $50kT$
iv	+	Liquid core and solid shell (figure 1(c))	Transition criterion
	♦	Liquid core and solid shell (figure 1(c))	Transition criterion and energy barrier less than $50kT$

5.2. Liquid to solid–liquid transition modes

Analogously, we start from the liquid particle at high T and then decrease T, at fixed R and x_0, to find the liquidus lines. Again, we see that a similar reasoning is applied to the modes of crystallization of an initially liquid Cu–Ni nanoparticle. Figure 3 summarizes the result of our analysis. It is worth noting that, at the transition criterion, in the case of configuration liquid core and solid shell (figure 1(c)), the energy barrier is super-high and corresponds to the appearance of nearly one atomic shell. Moreover, we see that, at the transition criterion, this is the polymorphic transition (polymorphic crystallization) when $x_n = x_p = x_0$. So, only great supersaturation, when the energy barrier is less than $50kT$, may lead to the nucleation in mode iv (denoted by the symbols ♦ and shown in figure 3 by the lowest curve at nearly unit compositions x_0).

Here the thermodynamically most probable mode is the mode v (denoted by the symbols ∇ and Δ in figure 3 and table 2), where the core is solid and the shell is liquid. Thus, we obtained that the new phase (solid part) appears in the internal part of the nanoparticle, in the core.

It is not obvious that solidification could take place in the centre part of the nanoparticle first. This means that in the thermodynamic limit the equilibrium structure of the Cu–Ni nanoparticles is a solid core containing a liquid shell. This is not a kinetic effect; this is thermodynamic effect. In this respect, we would like to mention the recent molecular dynamics simulations (based on the semiempirical embedded-atom method) of the freezing of gold nanodroplets, in which solidification starts at the surface when the final structure is icosahedral [29]. However, it is known that in icosahedra internal atoms are strongly compressed, so that the inner part of the cluster is not especially stable. It is the aim of our future works to look at the effects of shape and kinetics.

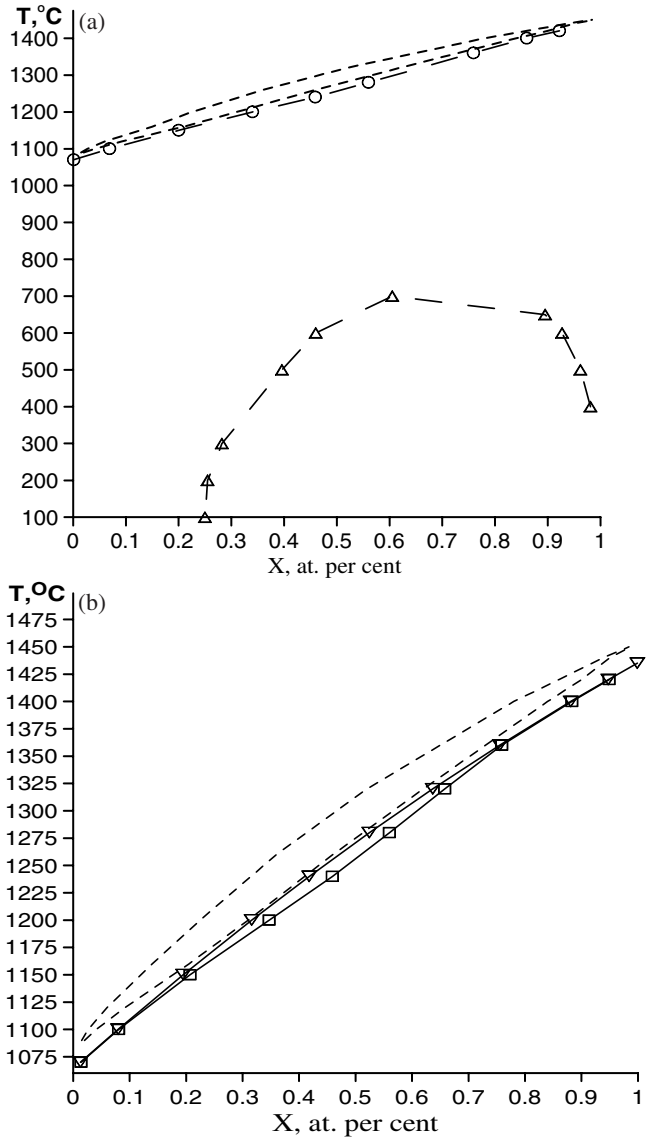

Figure 4. Solubility diagrams in the Cu–Ni nanosystem at $R_1 = 3 \times 10^{-8}$ m: (a) ○—solidus line; △—liquidus curve; (b) □—solidus line (which is formally equivalent to ○ in figure 2); ▽—liquidus curve (which is formally equivalent to + in figure 3). Dashed lines indicate the solidus and liquidus curves in the bulk Cu–Ni system.

5.3. Size-induced solubility diagram

Let us now apply the mentioned optimization procedure to the results shown in figures 2, 3 and plot the lines of solubility. The result of such a procedure for a Cu–Ni nanoparticle is presented in figure 4 for the case $R_1 = 3 \times 10^{-8}$ m.

In figure 4(a) (at fixed T, R and other parameters) only the solubility x_0 is shown, corresponding simultaneously to the:

- transition criterion,
- minimal nucleation barrier $\Delta G^* \leqslant 50kT$,
- minimal supersaturation of the treated system, when different values of x_{0i} exist (x_0 is taken to be closer to the field of the single phase state in the diagram).

In figure 4(b) we reduce the condition for minimal nucleation barrier $\Delta G^* \leqslant 50kT$. Here (at fixed T, R and other parameters) only the solubility x_0 remains, corresponding simultaneously to the:

- transition criterion,
- minimal supersaturation of the treated system, when different values of x_{0i} exist (x_0 is taken to be closer to the field of the single phase state in the diagram).

We see that new effects appear: (1) the effective width of the diagram decreases: the two-phase field narrows and even collapses the solidus and liquidus branches to a line for compositions about 0 and 1 (figure 4(b)); (2) there exists the possibility of the overlap and intersection of the solidus and liquidus in the solubility diagram (figure 4(a)); (3) the forms of the solubility curves in the diagram change; (4) the solubility diagram shifts down to lower temperatures, as compared to bulk state diagram; that is, it is size-dependent (figure 5).

Furthermore, we see that the overlap of liquidus and solidus lines is absent if the condition of minimal nucleation barrier $\Delta G^* \leqslant 50kT$ is absent. When the condition $\Delta G^* \leqslant 50kT$ is absent, we see the collapse of the solidus and liquidus (figure 4(b)) to a line for compositions about 0 and 1. In principle, the condition $\Delta G^* \leqslant 50kT$ corresponds to equation (16) and characterizes the experimental, possible kinetic behaviour of the system. From this, the thermodynamically correct result is shown in figure 4(b), whereas experimentally observed one may be as in figure 4(a).

It can be shown from general thermodynamic arguments that the solubility limits may be essentially varied by the geometry of the nanosystem and composition dependence of the surface energies at the interface as well as in the interphase boundary between the solid and liquid. Hereby the effective width of the two-phase interval on temperature–composition state diagram may increase or even decrease compared with the bulk case [13]. In our case we observe a narrowing of the two-phase field.

It is worth noting that the solidus and liquidus lines indicate only the start of melting and freezing but not the two-phase equilibrium. In another words, the lever rule for mass conservation does not work for the liquidus and solidus curves.

In infinite (bulk) material the solubility and the equilibrium curves coincide. So, the solubility diagram (at $R = \infty$) is the phase diagram.

To see the effect of size on the shape of the solubility curve, we present figure 5(b), where only liquidus curves are shown for three different sizes.

6. Concluding remarks

The classical nucleation theory has been applied to nanosystems in earlier publications. As has been pointed out, such modification takes into account the depletion effect. In previous works, we modified the notions ‘solidus’, ‘liquidus’ and outlined the new notions of a ‘solubility diagram’. In the present work, we used these results and the notion of a size-induced ‘solubility diagram’ to discuss the particular case of the Cu–Ni nanosystem.

For the first time, to our knowledge, we show the solubility diagram of a real Cu–Ni system and new possible effects such as the intersection of solidus and liquidus. The increase of the sizes leads to the vanishing of this last effect.

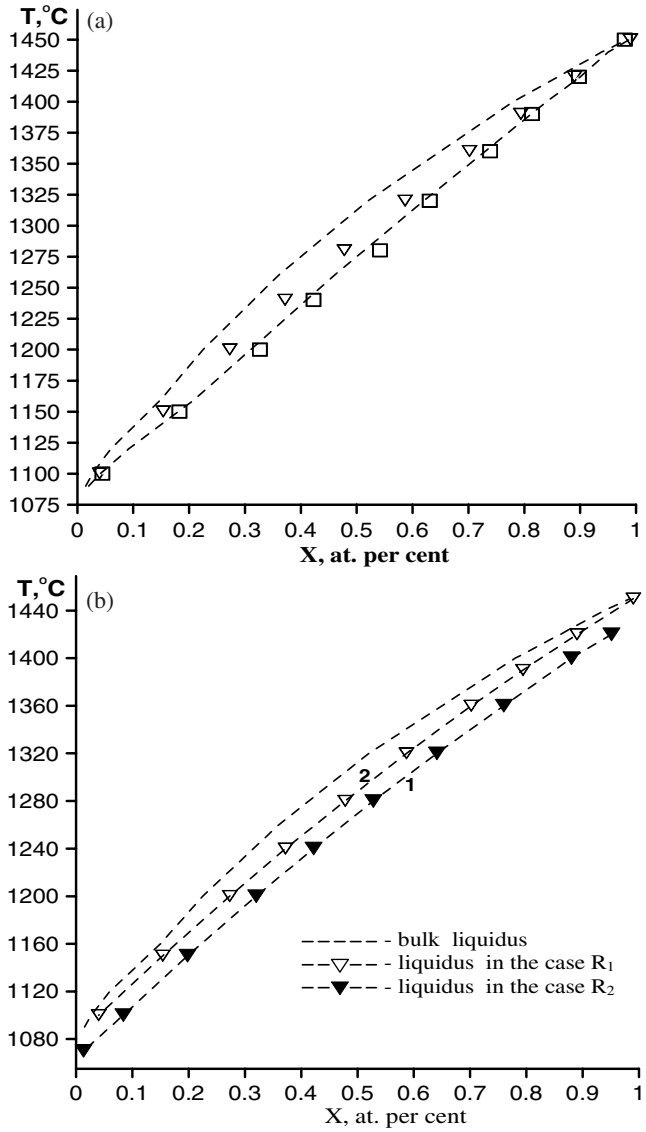

Figure 5. Effect of size and solubility diagram in the Cu–Ni nanosystem: (a) at $R_2 = 30 \times 10^{-8}$ m (▽—liquidus, □—solidus); (b) shifting and changing of the shape of solubility line—liquidus. Dashed lines indicate the solidus and liquidus curves in the bulk Cu–Ni system. $R_1 = 3 \times 10^{-8}$ m.

In accordance with the previously revised notions, we obtained that the size-induced solidus and liquidus lines indicate only the start of melting and freezing but not the two-phase equilibrium.

The present discussion is restricted to the cases where faceting plays no important role. Nucleation can proceed at the external boundary of a nanoparticle as well. Although the shape is considered here to be spherical-like, in our forthcoming analysis we want to take into account the effects of shape and chemical environment on melting and freezing temperatures. It is expected that the shape would play an important role in these processes.

Also, the possible size and temperature dependence of specific surface energies is not considered here. The corresponding modification of the present model will be discussed elsewhere.

Acknowledgments

The work was supported by the International Association for Promotion of Cooperation with Scientists from New Independent States of the former Soviet Union (Intas Ref. No: 03-55-1169). One of the authors (AS) appreciates the hospitality of the University of Mons-Hainaut, Belgium, where he worked currently under the INTAS Programme.

References

[1] Buffat Ph and Borel J P 1976 *Phys. Rev.* A **13** 2287
[2] Couchman P R and Jesser W A 1977 *Nature* **269** 481
[3] Petrov Y I 1982 *Physics of Small Particles* (Moscow: Science)
[4] Nagaev E L 1992 *Usp. Fiz. Nauk* **162** 50
[5] Rusanov A I 1978 *Phasen gleichgewichte und Grenzflaecheners cheinungen* (Berlin: Akademie-Verlag)
[6] Ulbricht H, Schmelzer J, Mahnke R and Schweitzer F 1988 *Thermodynamics of Finite Systems and Kinetics of First-Order Phase Transitions* (Leipzig: BSB Teubner)
[7] Gusak A M and Shirinyan A S 1999 *Met. Phys. Adv. Tech.* **18** 659
[8] Liang L H, Liu D and Jiang Q 2003 *Nanotechnology* **14** 438
[9] Wautelet M 1992 *Nanotechnology* **3** 42
[10] Shirinyan A S and Gusak A M 2004 *Phil. Mag.* A **84** 579
[11] Jesser W A, Shneck R Z and Gille W W 2004 *Phys. Rev.* B **69** 144121
[12] Shirinyan A S and Wautelet M 2004 *Nanotechnology* **15** 1720
[13] Shirinyan A S, Gusak A M and Wautelet M 2005 *Acta Mater.* **53** 5025
[14] Mottet C *et al* 2005 *Phys. Rev. Lett.* **95** 035501
[15] Rossi G *et al* 2005 *J. Chem. Phys.* **122** 194309
[16] Baletto F and Ferrando R 2005 *Rev. Mod. Phys.* **77** 371
[17] Huang S P and Balbuena P B 2002 *J. Phys. Chem.* B **106** 7225
[18] Zernike J 1955 *Chemical Phase Theory* (Deventer-Antwerp-Djakarta: N. V. Uitgevers-Maatschappij-AE.E. Kluwer)
[19] Matienseen W and Warlimont H (ed) 2005 *Springer Handbook of Condensed Matter and Materials Data* (New York: Springer)
[20] Christian J W 1965 *Theory of Transformation in Metals and Alloys* (New York: Pergamon)
[21] Seitz F 1940 *The Modern Theory of Solids* (New York: McGraw-Hill)
[22] Gibbs J W 1928 *The Collected Works of J.Willlard Gibbs: In Two Volumes* (New York: Longmans, Green and Co.)
[23] Weast R C (ed) 1986–1987 *CRC Handbook of Chemistry and Physics* 67th edn (Boca Raton, FL: CRC Press)
[24] Shackelford J F and Alexander W (ed) 2001 *CRC Material Science and Engineering Handbook* 3rd edn (Boca Raton, FL: CRC Press)
[25] Smithells C J and Brandes E A (ed) 1976 *Metal Reference Book.* 5th edn (London and Boston: Fulmer Research, Ltd./Butterworth)
[26] Jiang Q, Lu H M and Zhao M 2004 *J. Phys.: Condens. Matter* **16** 521
[27] Magomedov M N 2004 *Solid State Phys.* **46** 924
[28] Seitz F and Turnbull D (ed) 1965 *Solid State Physics. Advances in Research and Applications* vol 3 (New York: Academic)
[29] Nam H S *et al* 2002 *Phys. Rev. Lett.* **89** 275502